JOURNAL OF OPTOELECTRONICS AND ADVANCED MATERIALS Vol. 11, No. 10, October 2009, p. 1490 - 1493

Structural investigations of ion beam synthesized β-$FeSi_2$♣

CH. ANGELOV*, BL. AMOV, V. MIKLI[a], R. TRAKSMAA[a]
Institute for Nuclear Research and Nuclear Energy, Bulgarian Academy of Sciences, 72 Tzarigradsko Chaussee blvd., Sofia 1784, Bulgaria
[a] *Centre for Materials Research, Tallinn Technical University, Ehitajate 5, Tallinn 19086, Estonia*

High dose Fe ion implantation in n-type Si (100) was applied in order to fabricate the β-$FeSi_2$ phase. Two sets of samples, using two steps of ion implantation at energies of 60 plus 20 keV and 90 plus 25 keV, were performed, using different doses in the range $1x10^{16}$ – $5x10^{17}$ cm^{-2}. X-ray diffraction (XRD) spectra were used as a criterion for the formation of the β-$FeSi_2$ phase. The effects of the different doses, annealing temperature and annealing time on the surface morphology were investigated by scanning electron microscopy (SEM) and atomic force microscopy (AFM). The Fe depth distributions were simulated by SRIM code and the initial theoretical profiles were estimated.

(Received November 5, 2008; accepted December 15, 2008)

Keywords: Fe^+ implantation, β-$FeSi_2$ phase, X-ray diffraction, Atomic force microscopy

1. Introduction

Ion beam synthesis (IBS) is a non – equilibrium process and one of the most suitable techniques employed to form semiconducting silicides in a controllable and reproducible way. After the first successful fabrication of silicides by IBS [1], the formation of Si-based structures emitting light in the visible and infrared regions has attracted much attention. Iron is a low-solubility impurity in silicon (N ~ 10^{16} cm^{-3}). The synthesis of iron silicides has to be performed at Fe dopant concentrations greatly exceeding the level of equilibrium solubility in silicon. Among different phases in the Fe-Si system, semiconducting iron disilicide (β-$FeSi_2$) is of interest for creation of materials with new photoelectric (emitting in the 1.5 μm region, a transparency band for Si and SiO_2) and thermoelectric properties [2]. The conventional IBS for the formation of silicides consists of two steps: ion implantation of Fe ions into Si substrates followed by annealing. Several methods of annealing have been used for the preparation of silicides: conventional furnace annealing, rapid thermal annealing (RTA), laser annealing and pulsed ion-beam treatment [3-8]. Despite the number of investigations for preparation of iron silicides by IBS, only a few studies examine the formation of β-$FeSi_2$ via RTA.

In the present work, the effects of temperature and duration of the RTA process on β-$FeSi_2$ formation of Fe^+ implanted Si substrates are investigated.

2. Experimental details

Ion implantation was carried out in a type ILU-4 ion accelerator. In order to form precipitations or unburied surface layers, two-step $^{56}Fe^+$ ion implantations in n-type (100) Si wafers at energies of 60 keV plus 20 keV and 90 keV plus 25 keV were performed, using different doses, resulting in total doses of $1x10^{16}$ cm^{-2} to $5x10^{17}$ cm^{-2}. Some of the samples were rapid thermal annealed at 800 ^oC and 900 ^oC for two different times – 15 and 60 s. The β-$FeSi_2$ phase formation into the samples was studied by XRD analysis, using a Bruker AXS X-ray diffractometer, D5005, with Cu Kα radiation.

The surface morphology of the implanted and annealed samples was examined using a Jeol JSM-840A scanning electron microscope. More detailed images of the surface were obtained using a SMENA atomic force microscope (NT-MDT, Russia) in semi-contact mode in air. Non-contact ultrasharp cantilevers (MikroMasch) with a typical force constant of 17.5 N/m and a typical

♣ Paper presented at the International School on Condensed Matter Physics, Varna, Bulgaria, September 2008

curvature radius of the tip of about 10 nm were used for estimation of the surface roughness. All statistical parameters were calculated on 2x2 and 5x5 μm^2 areas, with NT-MDT NOVA Solver software.

The initial ^{56}Fe implantation profiles were simulated by the SRIM computer code [9].

3. Results and discussion

High dose Fe^+ implantation into Si substrates, followed by RTA, was used to fabricate iron silicide layers. The implantation conditions and annealing regimes are given in Table 1.

Table 1.Summary of the implantation and annealing conditions.

Sample	$^{56}Fe^+$, Energy, Doses
D_1	60 keV, 5x10^{15} cm^{-2} + 20 keV, 5x10^{15} cm^{-2}, annealed 900 ^{o}C, 60 sec
D_2	60 keV, 5x10^{16} cm^{-2} + 20 keV, 5x10^{16} cm^{-2}
D_{21}	60 keV, 5x10^{16} cm^{-2} + 20 keV, 5x10^{16} cm^{-2}, annealed 800 ^{o}C, 60 sec
D_3	60 keV, 1x10^{17} cm^{-2} + 20 keV, 1x10^{17} cm^{-2}
D_4	90 keV, 4x10^{17} cm^{-2} + 25 keV, 1x10^{17} cm^{-2}
D_5	90 keV, 4x10^{17} cm^{-2} + 25 keV, 1x10^{17} cm^{-2}, annealed 800 ^{o}C, 15 sec
D_6	90 keV, 4x10^{17} cm^{-2} + 25 keV, 1x10^{17} cm^{-2}, annealed 900 ^{o}C, 15 sec

The initial implantation profiles for the first set of the implanted samples, simulated by the SRIM computer code are shown in Fig. 1. In order to obtain precipitates (D_1, D_2 and D_3) or uniform β-$FeSi_2$ layers (D_4, D_5 and D_6), the peak concentration of Fe atoms has to exceed the value for the stoichiometric compound (2.6x10^{22} cm^{-3}). This requires suitable values of the energy and dose of the implanted ions.

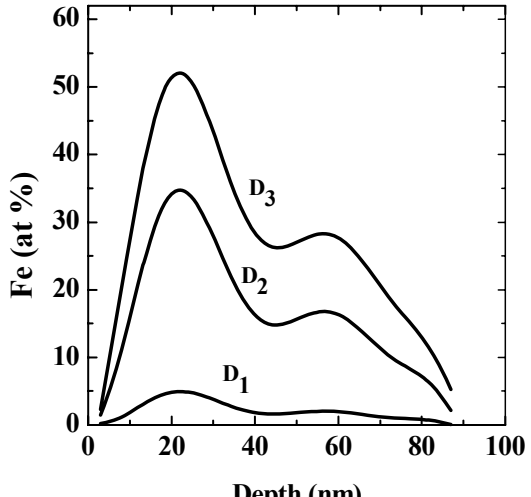

Fig. 1. Fe^+ implantation profiles for the first set of samples, simulated by SRIM.

For the first set of samples, ion implantation with energies of 60 and 20 keV was performed, using three different doses: D_1=5x10^{15}, D_2=5x10^{16} and D_3=1x10^{17} cm^{-2}, resulting in total doses of 1x10^{16} cm^{-2}, 1x10^{17} cm^{-2} and 2x10^{17} cm^{-2} respectively. The depth of the initially formed amorphous layer was calculated to be 98 nm, with a peak of implanted Fe atoms at 53 nm. Two samples (D_1 and D_2) were rapid thermal annealed at 800 and 900 ^{o}C. The XRD spectra of the Fe implanted and annealed samples are shown in Fig. 2.

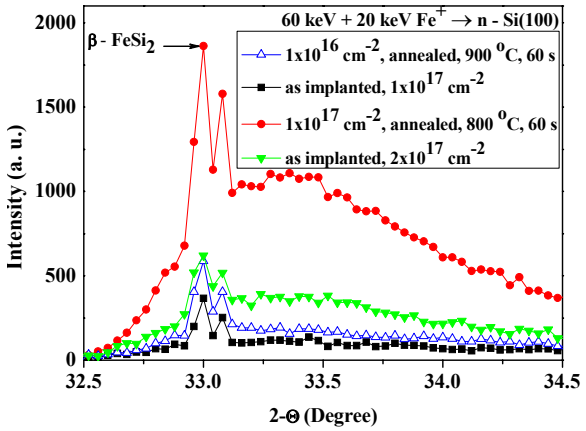

Fig. 2. XRD spectra of Fe samples implanted in Si with doses D_1, D_2 and D_3 and annealed .

One can see that the optimum condition for the formation of the β-$FeSi_2$ phase is implantation with a dose of 1x10^{17} cm^{-2}, followed by RTA at 800 ^{o}C for 60 s.

In the case of the second set of samples, 90 and 25 keV Fe^+ implantation was used with doses of 4x10^{17} cm^{-2} and 1x10^{17} cm^{-2} respectively, resulting in a total dose of 5x10^{17} cm^{-2} (Fig. 3).

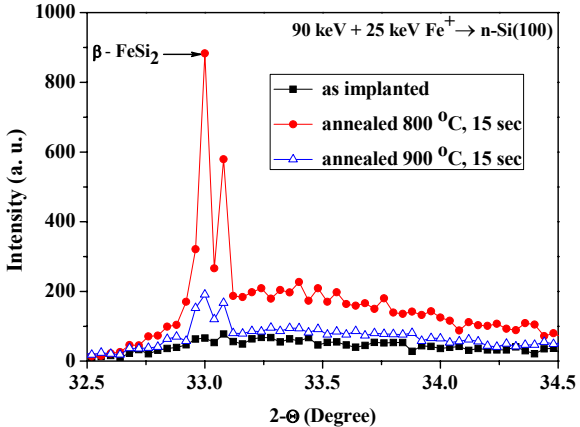

Fig. 3. XRD spectra of Fe implanted and annealed Si samples (D_4, D_5 and D_6).

The depth of the initially formed amorphous layer was calculated to be 170 nm with a peak of implanted Fe atoms at 66 nm [9]. Samples were annealed at 800 and 900 ^{o}C for 15 s. Again, the most suitable conditions for β-$FeSi_2$ phase formation detected by XRD are ion implantation followed by 800^{o}C annealing for 15 s. Further increasing of the annealing temperature up to 900 ^{o}C destroys the formed β-$FeSi_2$ phase.

β-$FeSi_2$ is a promising candidate for application in optoelectronics, and thus it is important to investigate the development of the surface morphology after ion implantation and subsequent annealing. SEM micrographs did not reveal significant structural changes up to sample D_5 (90 keV, 4x10^{17} cm^{-2} + 25 keV, 1x10^{17} cm^{-2}, annealed 800 ^{o}C, 15 sec). Fig. 4 shows a SEM microphotograph of sample D_6 (90 keV, 4x10^{17} cm^{-2} plus 25 keV, 1x10^{17} cm^{-2}, annealed 900 ^{o}C, 15 s). One can see that with increased annealing temperature, a mosaic structure develops.

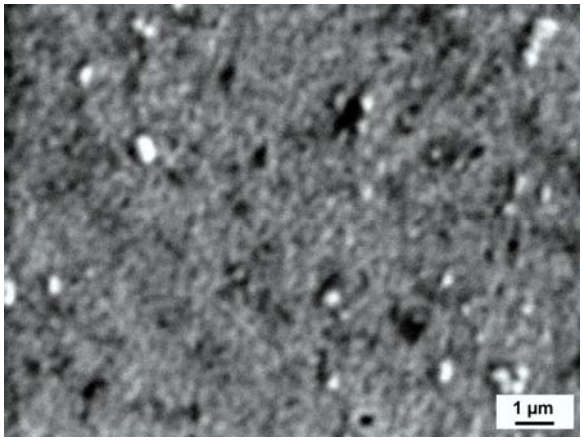

Fig. 4. SEM microphotograph of sample D_6

More detailed three-dimensional images of the Si surface after implantations and consecutive annealing were obtained by AFM. Fig. 5 shows AFM images of as-implanted (D_2 and D_3), and annealed (D_1 and D_{21}) samples. The calculated difference in the sputtering yields for Si (1.14 at/ion) and Fe (5.42 at/ion) for 60 keV Fe^+ implantation [9] led to preferential sputtering on the irradiated surface and development of cone-like structures. As a measure of the surface roughness of the samples, Root Mean Square (RMS) values were obtained. The AFM image for the first sample (D_1) was obtained from a 2x2 μm^2 area, all others from 5x5 μm^2 areas. Increasing the implanted dose from 1x10^{17} cm^{-2} (D_2) to 2x10^{17} cm^{-2} (D_3) results in a decrease of the roughness from 1.04 nm to 0.71 nm. The cone-like structures already formed at the lower dose start to destroy themselves during additional implantation. After annealing, a very strong increase in the surface roughness was observed. The values of the RMS roughness for D_1 and D_{21} were 8.57 nm and 5.71 nm respectively.

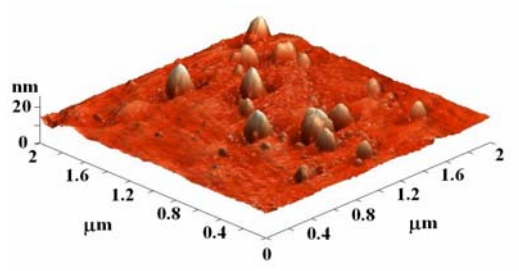

D_1

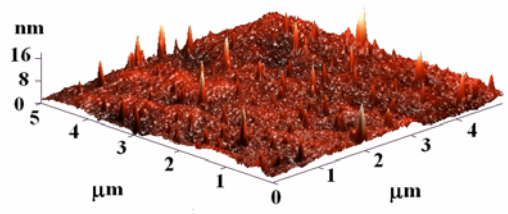

D_2

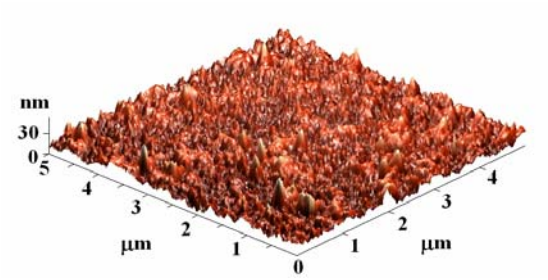

D_{21}

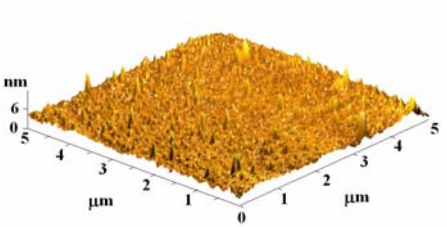

D_3

Fig. 5. AFM images of as-implanted (D_2 and D_3), and annealed (D_1 and D_{21}) samples

Fig. 6 shows AFM images for the second set of samples (D_4, D_5 and D_6). Again, due to the difference in sputtering yields for Si (1.13 at/ion) and Fe (5.32 at/ion) at 90 keV Fe^+ implantation [9] preferential sputtering occurs, resulting in the development of cone-like structures. The RMS value for the as-implanted sample is 1.53 nm.

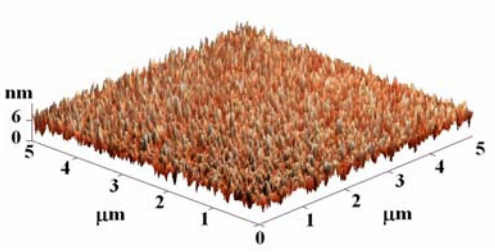

D_4

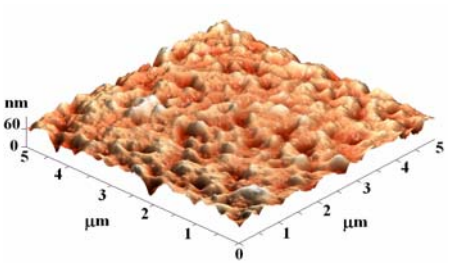

D_5

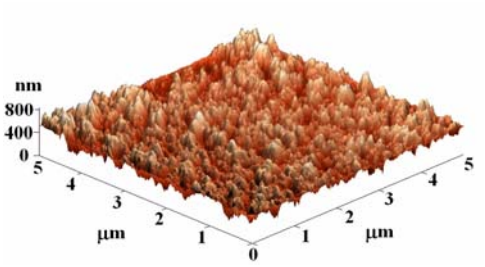

D_6

Fig. 6. AFM images of as-implanted (D_4), and annealed (D_5 and D_6) samples

Increasing the annealing temperature results in an increased RMS value for the surface roughness of 9.79 nm for the D_5 and 10.79 nm for the D_6 sample.

4. Conclusions

A non-equilibrium process - IBS - was used to fabricate the β-$FeSi_2$ phase in Si. The phase formation and the surface roughness of the implanted samples were strongly influenced by the implantation conditions and subsequent annealing. XRD spectra indicate that thermal annealing at 800 ^oC is the most favorable regime for the β-$FeSi_2$ phase formation.

Acknowledgements

This study was supported by ESF grant № G 7608.

References

[1] A. E. White, K. T. Short, R. C. Dynes, J. P. Garno, Appl. Phys. Lett. **50**, 95 (1987).
[2] Y. K. Hsu, J. J. Wang, C. S. Chang, S. C. Wang, Jpn. J. Appl. Phys. **41**, 6A, 3854, (2002).
[3] M. Sugiyama, Y. Maeda, Thin Solid Films **381**, 225 (2001).
[4] M. M. Mitan, D. P. Pivin, T. L. Alford, J. W. Mayer, Appl. Phys. Lett. **78**, 2727, (2001).
[5] R. M. Bayazitov, R. I. Batalov, I. B. Khaibullin, G. D. Ivlev, I. Dézsi, E. Kotai, J. Phys. D: Appl. Phys. **37**, 468 (2004).
[6] R. I. Batalov, R. M. Bayazitov, I. B. Khaibullin, E. I. Terukov, V. Kh. Kudoyarova, Nanotechnology **12**, 409 (2001).
[7] H. Katsumata, Y. Makita, N. Kobayashi, M. Hasegawa, H. Shibata, S. Uekusa, Thin Solid Films **281-82**, 252 (1996).
[8] Ch. Angelov, S. Georgiev, B. Amov, E. Goranova, V. Mikli, I. Dezsi, E. Kotai, J. Optoel. Adv. Materials **9**, .307 (2007).
[9] J. F. Ziegler, J. P. Biersack, SRIM 2008, www.SRIM.org.

*Corresponding author: hangelov@inrne.bas.bg